ELSEVIER

# Hydroesterification versus hydroformylation–acetalization of 1-hexene catalyzed by soluble carbonylrhodium complexes of pyridine ligands

Alvaro J. Pardey [a,*], Gabriela C. Uzcátegui [a], Fernando Hung-Low [a],
Angel B. Rivas [a], Jorge E. Yánez [a], Marisol C. Ortega [a], Clementina Longo [b],
Pedro Aguirre [c], Sergio A. Moya [d]

[a] *Centro de Equilibrios en Solución, Escuela de Química, Facultad de Ciencias, Universidad Central de Venezuela, Caracas, Venezuela*
[b] *Centro de Investigación y Desarrollo de Radiofármacos, Facultad de Farmacia, Universidad Central de Venezuela, Caracas, Venezuela*
[c] *Departamento de Química Inorgánica y Analítica, Facultad de Ciencias Químicas y Farmacéuticas, Universidad de Chile, Santiago, Chile*
[d] *Departamento de Química Aplicada, Facultad de Química y Biología, Universidad de Santiago de Chile, Santiago, Chile*

## Abstract

The rhodium(I) complexes, *cis*-[Rh(CO)$_2$(amine)$_2$](PF$_6$) (amine = pyridine, 2-picoline, 3-picoline, 4-picoline, 3,5-lutidine or 2,6-lutidine) dissolved in methanol under carbon monoxide atmosphere are effective catalysts for the hydroesterification and hydroformylation–acetalization of 1-hexene. In the presence of these soluble complexes, 1-hexene, CO and methanol give methyl-heptanoate and 1,1-dimethoxy-heptane as major products, and minor amounts of heptanal. The acetal product comes from the nucleophilic addition reaction of the methanol with the formed heptanal. Gaseous by-products (H$_2$ and CO$_2$) from the catalysis of the water–gas shift reaction (WGSR) are also observed. The reaction products distribution depends on the nature of the coordinated amine to the rhodium center. The effects of the reaction variables such as CO pressure, temperature, catalyst concentration, 1-hexene/Rh molar ratio and reaction medium, were also examined. These data are discussed in terms of catalytic cycles, and it is concluded that common Rh–H catalytic species are involved.
© 2005 Published by Elsevier B.V.

*Keywords:* Reppe synthesis; Rhodium complexes; 1-Hexene; Hydroesterification; Hydroformylation–acetalization; Water–gas shift reaction

## 1. Introduction

It is well known the synthesis of oxygenated organic products by reaction of an olefinic substrate with CO and water or alcohols (Z = −OH or −OR, Eq. (1)) in the presence of transition metal complexes to give carboxylic acids (hydrocarboxylation reaction) or their esters (hydroesterification reaction), respectively [1]. This type of Reppe synthesis has received considerable attention and it is the subject of a recent review [2]:

$$RHC=CH_2 + CO + ZH \rightarrow RH_2C-CH_2C(=O)-Z \qquad (1)$$

Recently, some examples of Reppe synthesis promoted by homogeneous and immobilized rhodium [3–6], cobalt [7], water soluble-palladium [8] and ruthenium [9] catalysts and acetal formation under hydroformylation conditions in the presence of alcohols [10,11] have been reported.

The naphtha, which constitutes a stream extracted from crude oil, is formed by combinations of C$_5$–C$_8$ saturated and unsaturated hydrocarbons. The light naphtha is used principally for the formulation of gasoline. The olefin content in the naphtha is ca. 43.5% [12] and it must be less than 6% in volume, according to the standard regulation. Higher amounts of these compounds in the gasoline induces chemical reactions in the combustion motors of the vehicles at high working temperatures, giving solid particles, which can block the injector and the valve system of the motor, therefore diminishing its efficiency.

* Corresponding author. Tel.: +58 212 6051225; fax: +58 212 4818723.
*E-mail address:* apardey@strix.ciens.ucv.ve (A.J. Pardey).

A heterogeneous catalytic hydrogenation process is employed to reduce the olefin content of the naphtha to saturated hydrocarbons. However, this process has some limitations, which are associated with the high consumption of the expensive $H_2$ and production of low octane content gasoline. Further, with the objective of increasing the octane content in the gasoline for improved emissions quality, diverse oxygenated additives like methyl-*tert*-butylether or -*tert*-ammilmethylether commonly are added in commercial gasoline.

The Reppe reaction catalyzed by transition metal complexes could be in principle applied for improving the low stream refinery (LSR). That process could increase the octane content of the gasoline by allowing in situ transformation of the olefins already present in this type of oil in oxygenated compounds with high aggregated value, likes esters, aldehydes, and acetals, among others. Additionally this could be carried out in one step avoiding the expensive catalytic hydrogenation.

Soluble cationic carbonylrhodium(I) complexes of pyridine and related ligands have demonstrated their ability to be applied as catalysts for the WGSR [13], carbonylation of methanol [14], reduction of nitrobenzene [15] and oligomerization of CO/ethylene [16]. However, to the best of our knowledge, a detailed study of the kinetics and mechanisms of soluble metal rhodium complexes on the catalytic hydroesterification and hydroformylation–acetalization of olefins has not yet been reported.

Continuing our work on *cis*-[Rh(CO)$_2$(amine)$_2$](PF$_6$) complexes, we report here the influence of the nature of the coordinated amine as well as the effect of variations in reaction parameters on catalytic hydroesterification and hydroformylation–acetalization of 1-hexene in methanol by these rhodium(I) complexes and the mechanistic implications. Furthermore, typical naphtha contains about 33% of 1-hexene among the other olefins and for that reason it was used as a model molecule in this study.

## 2. Experimental

### 2.1. Materials and instrumentation

Pyridine (py), methyl pyridines (2-picoline (2-pic), 3-picoline (3-pic), and 4-picoline (4-pic)) and dimethyl pyridines (3,5-lutidine (3,5-lut) and 2,6-lutidine (2,6-lut)) were obtained from Aldrich and distilled over KOH. Methanol, ethanol and 1-hexene (Aldrich) were distilled prior to use. Water was doubly distilled. All gas mixtures He/H$_2$ (91.4%/8.6%, v/v), CO/CH$_4$ (95.8%/4.2%, v/v) and CO/CH$_4$/CO$_2$/H$_2$ (84.8%/5.1%/5.3%/4.8%, v/v) were purchased from BOC Gases and were used as received. The complexes of the type *cis*-[Rh(CO)$_2$(amine)$_2$](PF$_6$) (amine = 4-pic, 3-pic, 2-pic, py, 3,5-lut or 2,6-lut) were synthesized and characterized as reported by Denise and Pannetier [17] and their IR spectra in chloroform demonstrated their identity

and purity (two strong bands in the $\nu_{(CO)}$ region at 2095 and 2020 cm$^{-1}$). These complexes will be referred as Rh(amine)$_2$ complexes.

Gas samples analyses from catalysis and kinetics runs were performed as described in detail previously [18] on a Hewlett-Packard 5890 Series II programmable (Chem-Station) gas chromatograph fitted with a thermal conductivity detector. The column employed was Carbosieve-B (80–100 mesh) obtained from Hewlett-Packard and using the He/H$_2$ mixture as the carrier gas. Analyses of liquid phase were done on a Hewlett-Packard 5890 Series II programmable gas chromatograph fitted with a HP-1 (methyl silicone gum, 50 m × 0.323 mm × 0.17 µm) column and flame ionization detector, and using He as the carrier gas. A Varian Chrompack 3800 programmable gas chromatograph fitted with a CP-Sil-8-CB (phenyldimethylpolysiloxane) (30 m × 0.250 mm) column and a Varian Chrompack, Saturn 2000 mass selective detector were used to confirm the identity of the organic reaction products at the end of each run. Also the organic products were separated by column chromatography and analyzed by $^{13}$C and $^{1}$H NMR in a Jeol Eclipse 270 NMR spectrometer.

### 2.2. Catalyst testing

Catalytic runs were carried out in all-glass reactor vessels consisting of a 100 mL round bottom flask connected to an "O" ring sealed joint to a two-way Rotoflow Teflon stopcock attached to the vacuum line. In a typical run, a given amount of the catalyst (5 × 10$^{-5}$ mol), 0.4 mL (3 × 10$^{-3}$ mol) of 1-hexene and 10 mL of methanol (0.24 mol) were added to the glass reactor vessel, and then the mixture was degassed by three freeze–pump–thaw cycles. The reaction vessel was charged with CO/CH$_4$ mixture at the desired CO partial pressure (0.7 atm at 25 °C, but 0.9 atm at 100 °C), and then suspended for 5 h in a circulating thermostated glycerol oil bath set at 100 °C. The specified temperature was maintained at ±0.5 °C by continuously stirring the oil bath, as well as the reaction mixture with Teflon-coated magnetic stirring bars. At the end of the reaction time gas samples (1.0 mL) were taken by means of gas tight syringes from the gaseous phase above the mixture and analyzed by GC. The CH$_4$ was used as internal standard to allow calculation of absolute quantities of CO consumed and H$_2$ and CO$_2$ produced. In addition, calibration curves were prepared periodically for CO, CH$_4$, H$_2$, and CO$_2$, and analyzing known mixtures checked their validities. Moreover, liquid samples were removed and analyzed by GC and GC–MS. Peak position of various reaction products were compared and matched with the retention times of authentic samples. The amounts of organic products were determined by using the response factor method for gas chromatographic analyses [19].

Catalytic runs under supra-atmospheric pressures were carried out in a 150 mL mechanically stirred stainless steel Parr autoclave charged with a given amount

$((1–30) \times 10^{-5} \text{ mol})$ of the *cis*-[Rh(CO)$_2$(4-pic)$_2$](PF$_6$) complex, variable amounts of 1-hexene, 10 mL of methanol and pressurized with CO (15–55 atm at 100 °C). The autoclave was placed in a temperature-controlled heating device at typically $100 \pm 1$ °C and mechanically stirred for a given time. These pressures and temperatures were chosen as an average from previously reported systems [20]. At the end of the reaction time gas and liquid samples were taken and analyzed by GC. Identity of those products was also confirmed by GC–MS.

## 3. Results and discussion

### 3.1. General aspects

The Rh(amine)$_2$ catalysts were investigated as precursors for the catalytic reactions of 1-hexene/CO with methanol. These catalytic systems are known to be active for 1-hexene hydroesterification (Eq. (2)) and hydroformylation (Eq. (3)), the WGSR (Eq. (4)) and the acetalization of the formed heptanal with alcohols (Eq. (5)). Also, traces ($\sim$1%) of products coming from isomerization of 1-hexene under catalysis conditions were observed.

The relative extent of the competing catalytic reactions can be established by comparing the amounts of the products. The results are shown in Table 1. Further control experiments show that activity toward the hydroesterification and the hydroformylation–acetalization of 1-hexene under CO was not observed when the mixture of methanol with 1-hexene was tested under similar experimental conditions in the absence of any of these Rh(amine)$_2$ catalysts.

On the other hand, 1-hexene was adopted as a model substrate because it represents ca. 33% of the olefin fraction on typical naphtha:

$$CH_3-(CH_2)_3-CH=CH_2 + CO + CH_3OH$$
$$\xrightarrow{Rh(amine)_2} CH_3-(CH_2)_5-C(=O)OCH_3 \qquad (2)$$

$$CH_3-(CH_2)_3-CH=CH_2 + 2CO + H_2O$$
$$\xrightarrow{Rh(amine)_2} CH_3-(CH_2)_5-C(=O)H + CO_2 \qquad (3)$$

$$CO + H_2O \xrightleftharpoons{Rh(amine)_2} CO_2 + H_2 \qquad (4)$$

$$CH_3-(CH_2)_5-C(=O)H + 2ROH$$
$$\rightarrow CH_3-(CH_2)_5-C(OR)_2H + H_2O \qquad (5)$$
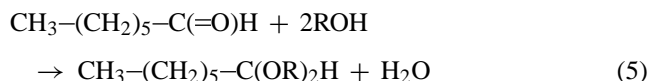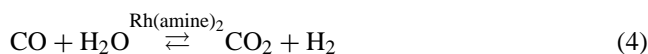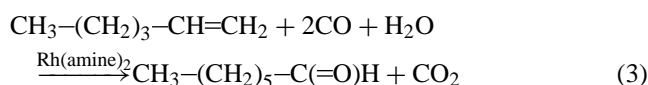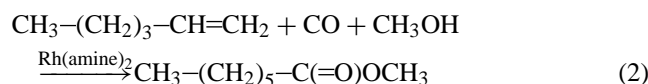
### 3.2. Hydroesterification and hydroformylation–acetalization catalysis

Table 1 summarizes the results of the catalytic hydroesterification and hydroformylation–acetalization of 1-hexene by the Rh(amine)$_2$ complexes dissolved in methanol under CO atmosphere. $^1$H NMR, GC and GC–MS analyses of the liquid phases identified methyl-heptanoate, heptanal and 1,1-dimethoxy-heptane coming from the 1-hexene hydroesterification in methanol (Eq. (2)), hydroformylation (Eq. (3)), and the addition reaction between methanol and the formed heptanal (Eq. (5)), respectively [22].

Control experiments in the absence of any of the soluble catalysts showed formation of 1,1-dimethoxy-heptane when a 1.0 mL sample of heptanal is placed in contact with 10 mL of methanol under $P$(CO) = 0.9 atm at 100 °C by 4 h. The heptanal conversion under the above-described conditions is 21%. Accordingly, Table 1 does not record the TF of acetal production due to its stoichiometric formation. However, in presence of the soluble Rh(4-pic)$_2$ complex ([Rh] = 0.022 g (5 × 10$^{-5}$ mol)) catalysis formation of 1,1-dimethoxy-heptane is observed when a 1.0 mL sample of heptanal (7 × 10$^{-3}$ mol) is placed in contact with 10 mL of methanol under $P$(CO) = 0.9 atm at 100 °C for 4 h. The heptanal conversion under the above-described conditions slightly increases from 21 to 36%. However, attempts to measure the catalytic impact on the production of these acetals by the others Rh complexes were not made.

Table 1
WGSR, hydroesterification and hydroformylation–acetalization of 1-hexene in methanol, catalyzed by the *cis*-[Rh(CO)$_2$(amine)$_2$](PF$_6$) complexes[a]

| Amine (p$K_a$)[b] | [CO$_2$] (total) (mol × 10$^{-5}$) | TF(CO$_2$)[c] total | [H$_2$] (mol × 10$^{-5}$) | TF(H$_2$)[c] | [MH][d] (mol × 10$^{-5}$) | TF(MH)[c,d] | [Heptanal] (mol × 10$^{-5}$) | [1,1-DMH][d] (mol × 10$^{-5}$) |
|---|---|---|---|---|---|---|---|---|
| Pyridine (5.27) | 14.2 | 17 | 4.9 | 6 | 5.6 | 7 | 0.2 | 7.5 |
| 3-Picoline (5.52) | 16.7 | 20 | 4.4 | 5 | 7.3 | 9 | 0.2 | 10.8 |
| 2-Picoline (5.97) | 10.8 | 13 | 4.5 | 5 | 5.0 | 6 | 0.2 | 5.0 |
| 4-Picoline (6.00) | 12.5 | 15 | 4.8 | 5 | 11.8 | 14 | 0.2 | 7.5 |
| 3,5-Lutidine (6.63) | 14.2 | 17 | 4.4 | 5 | 13.0 | 16 | 0.2 | 8.4 |
| 2,6-Lutidine (6.75) | 11.7 | 14 | 5.3 | 7 | 17.2 | 21 | 0.2 | 5.0 |

[a] [Rh] = (5 × 10$^{-5}$ mol), [1-hexene] = 0.4 mL (3 × 10$^{-3}$ mol), 1-hexene/Rh = 64, 10 mL (0.24 mol) of methanol, $P$(CO) = 0.9 atm at 100 °C for 4 h.
[b] From Ref. [21].
[c] TF(product) = [(mol of product/mol of Rh) × (rt)] × 24 h, where (rt) = reaction time in hours. Experimental uncertainty < 10%.
[d] MH = methyl-heptanoate; DMH = dimethoxy-heptane.

The results in methanol show that TF(methyl-heptanoate)/24 h (TF(MH)/24 h) values depend on the nature of the coordinated amine and decrease in the following order: 2,6-lut > 3,5-lut > 4-pic > 3-pic > py > 2-pic. Accordingly, the catalytic hydroesterification of 1-hexene by Rh(amine)$_2$ complexes is influenced principally by the basic nature of the amine. Thus, the Rh(2,6-lutidine)$_2$ system is the most active. The reverse order observed in the case of the Rh(2-pic)$_2$ system is due to the steric hindrance factor which overwhelms the electronic one. It is interesting to see on the Rh(2,6-lut)$_2$ system that the steric hindrance factor does not overwhelm the electronic factor even though the 2,6-lutidine amine is the most sterically hindered of all of the amines tested in this work.

However, the steric factor seems to control the observed tendency on the catalytic hydroformylation–acetalization of 1-hexene by these Rh(amine)$_2$ systems.

Based on the amounts of methyl-heptanoate, heptanal and 1,1-dimethoxy-heptane formed (Table 1) it can be observed that the hydroesterification of 1-hexene is more favored than hydroformylation–acetalization reactions by a factor ranging from 1.5- to 3.3-fold for the more basic amines, namely: 3,5-lut (60% yield of ester), 4-pic (61% yield of ester) and 2,6-lut (77% yield of ester). However, the opposite tendency is observed when the amines are the less basic pyridine: (42% yield of ester) and 3-pic (40% yield of ester); being the 2-pic (49% yield of ester) in the borderline. The yields of ester, aldehyde and acetal were calculated based on GC data and by considering the total yields of the above three oxygenated products equal to 100%. These results suggested that the electronic factor induced by the methyl groups of the coordinated amine influences the rate of these two competing reactions, hydroesterification versus hydroformylation–acetalization.

### 3.3. WGSR catalysis

Since the early work of Reppe, the relationship between WGSR and olefin hydroesterification/hydroformylation with CO/H$_2$O in alkaline solution has been recognized [23]. All of these Rh(amine)$_2$ soluble complexes, are also active for the catalysis of the WGSR under the conditions required for the catalytic hydroesterification/hydroformylation–acetalization of 1-hexene. Even though reagents and solvents used were pre-dried, formation of water occurred via acetal formation (Eq. (5)). GC analyses of the gas phase of the catalytic runs allowed the identification of H$_2$ and CO$_2$ as sole gaseous products. The H$_2$ and certain amount of CO$_2$ come from the WGSR. Another portion of the CO$_2$ produced comes from the catalytic hydroformylation of 1-hexene under CO/H$_2$O (Eq. (3)) and the total CO$_2$ mass balances both (Eqs. (3) and (4)).

Further, a control experiment shows no WGSR activity in the absence of any of soluble Rh(amine)$_2$ catalysts under similar reaction conditions. The results in methanol show that TF(H$_2$) values are low and almost similar, suggesting that the nature of the amine does not control WGSR rates in these systems. A different trend was observed in the catalysis of the WGSR by cis-[Rh(CO)$_2$(amine)$_2$](PF$_6$) dissolved in 80% aqueous pyridine or substituted pyridines. For example the TF(H$_2$) decreased from 4-picoline (80) to 2,6-lutidine (1) under the following catalysts conditions: [Rh] = 10 mM, 10 mL of 80% aqueous amine under $P$(CO) = 0.9 atm at 100 °C. In those Rh(amine)$_2$/aqueous amine systems the steric factor controls the rate of H$_2$ and CO$_2$ formation [13].

### 3.4. Kinetics studies

The following kinetics studies were made using the Rh(4-pic)$_2$ system despite the Rh(2,6-lut)$_2$ was the most active for the hydroesterification reaction. The reason lies in the better stability of the cis-[Rh(CO)$_2$(4-pic)$_2$](PF$_6$) complex in comparison to cis-[Rh(CO)$_2$(2,6-lut)$_2$](PF$_6$), which tends to decompose in relatively short times on air. Therefore, for the purpose of kinetics studies we would rather work with one of the more highly active and more robust complex, namely cis-[Rh(CO)$_2$(4-pic)$_2$](PF$_6$).

For the Rh(4-pic)$_2$ system the effects of varying the carbon monoxide pressure $P$(CO), the temperature $T$, the rhodium concentration [Rh], and the 1-hexene/Rh molar ratio S/C on WGSR, hydroesterification and hydroformylation–acetalization of 1-hexene in methanol were explored.

Table 2
The effects of the carbon monoxide pressure variation on WGSR, hydroesterification and hydroformylation–acetalization of 1-hexene in methanol, catalyzed by the cis-[Rh(CO)$_2$(4-pic)$_2$](PF$_6$) complex[a]

| $P$(CO) (atm) | [CO$_2$] (total) ($\times 10^{-5}$ mol) | TF(CO$_2$)[b] total | [H$_2$] ($\times 10^{-5}$ mol) | TF(H$_2$)[b] | [MH][c] ($\times 10^{-5}$ mol) | TF(MH)[b,c] | [Heptanal] ($\times 10^{-5}$ mol) | [1,1-DMH][d] ($\times 10^{-5}$ mol) |
|---|---|---|---|---|---|---|---|---|
| 15 | 192.1 | 231 | 44.3 | 55 | 23.1 | 27 | 2.2 | 149.0 |
| 25 | 198.0 | 238 | 61.1 | 73 | 44.0 | 53 | 8.8 | 124.3 |
| 35 | 215.0 | 258 | 74.3 | 89 | 41.2 | 49 | 8.0 | 134.8 |
| 45 | 256.2 | 307 | 92.0 | 110 | 28.9 | 35 | 3.1 | 163.4 |
| 55 | 292.3 | 351 | 101.6 | 122 | 21.1 | 25 | 0.8 | 193.0 |

[a] [Rh] = 0.022 g (5 × 10$^{-5}$ mol), [1-hexene] = 0.4 mL (3 × 10$^{-3}$ mol), 1-hexene/Rh = 64, 10 mL (0.24 mol) of methanol, $T$ = 100 °C for 4 h.
[b] TF(product) = [(mol of product/mol of Rh) × rt] × 24 h, where rt = reaction time in hours. Experimental uncertainty < 10%.
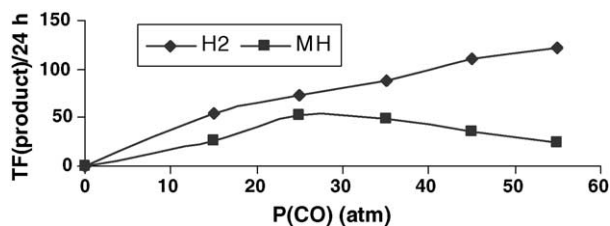[c] MH = methyl-heptanoate.
[d] DMH = dimethoxy-heptane.

Fig. 1. A plot of TF(product)/24 h vs. $P(CO)$: ($\blacklozenge$) hydrogen and ($\blacksquare$) methyl heptanoate. Reaction conditions: $[Rh] = 0.022$ g $(5 \times 10^{-5}$ mol), [1-hexene] $= 0.4$ mL $(3 \times 10^{-3}$ mol), 1-hexene/Rh = 64, 10 mL (0.24 mol) of methanol, $T = 100\,°C$ for 4 h. Lines drawn for illustrative purpose only.

### 3.4.1. Effect of the carbon monoxide pressure

The effect of varying the CO pressure for the Rh(4-pic)$_2$ system in methanol is summarized in Table 2. Fig. 1 shows the plot of TF(MH)/24 h values versus $P(CO)$. As can be inferred from Table 2 and Fig. 1, increase in $P(CO)$ from 15 atm is accompanied by improvement in the TF(MH)/24 h value, then reaches a maximum at $P(CO) = 25$ atm and starts decreasing at $P(CO) > 35$ atm. These findings indicate that the catalytic activity does not follow a linear dependence on $P(CO)$ in the range of 15–55 atm and suggest the formation of a less-active rhodium carbonyl species toward the hydroesterification reaction, at high CO pressure.

On the other hand, the total amounts of products coming from the hydroformylation–acetalization reaction starts increasing steadily in the 25–55 atm range at 100 °C, indicating that this reaction is first order in $P(CO)$ in the study range. Accordingly, while the hydroesterification reaction is disfavored at high $P(CO)$, the opposite occurs with the hydroformylation–acetalization reaction.

The plot of TF(H$_2$) values versus $P(CO)$ for $[Rh] = 5 \times 10^{-5}$ mol at 100 °C shown in Fig. 1, is almost linear, indicating that the reaction is first order in [CO] at this temperature in the 15–55 atm range. Based on the first order in [CO] we suggest a possible mechanism in that the rate-limiting step ($k_2$) is preceded by coordination of CO, e.g.:

$$[Rh]^+ + CO \xrightarrow{k_1} [Rh-CO]^+ \xrightarrow{k_2, H_2O} products \tag{6}$$



Fig. 2. The Arrhenius plot for hydroesterification catalysis. Reaction conditions: $[Rh] = 0.022$ g $(5 \times 10^{-5}$ mol), [1-hexene] $= 0.4$ mL $(3 \times 10^{-3}$ mol), 1-hexene/Rh = 64, 10 mL (0.24 mol) of methanol, $P(CO) = 25$ atm for 4 h.

The WGSR and hydroformylation–acetalization rate law for such behavior would be

$$rate = k_1 k_2 P(CO)[Rh]_{tot} \tag{7}$$

where $[Rh]_{tot} = [Rh]^+ + [Rh-CO]^+$ and $k_1$ includes the solubility of CO in the medium and $k_2$ the [solvent]. The above expression, Eq. (7) can be reduced to

$$TF(product) = k_1 k_2 P(CO) \tag{8}$$

where product = H$_2$, CO$_2$, heptanal or 1,1-dimethoxy-heptane.

For this kinetics model plots of TF(product) versus $P(CO)$ should be linear with slopes of $k_1 k_2$ and zero intercept. For example, the TF(H$_2$) plot versus $P(CO)$ is linear with nearly a zero intercept value as predicted by Eq. (8). Further, by plotting $\ln TF(H_2)$ versus $\ln P(CO)$ a slope with a value ca. 1 is observed.

### 3.4.2. Effect of the temperature

To determine the activation parameters for the WGSR, TF(H$_2$)/24 h values for the Rh(4-pic)$_2$ system were measured at various temperatures in the 100–140 °C range (Table 3). Fig. 2 displays the $\ln TF(MH)/24$ h values versus $1/T$ plot for $[Rh] = 5 \times 10^{-5}$ mol, [1-hexene] $= 0.4$ mL
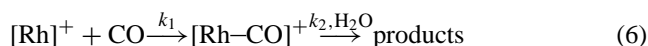
Table 3

The effect of the temperature variation on WGSR, hydroesterification and hydroformylation–acetalization of 1-hexene in methanol, catalyzed by the *cis*-[Rh(CO)$_2$(4-pic)$_2$](PF$_6$) complex[a]

| $T$ (°C) | [CO$_2$] (total) ($\times 10^{-5}$ mol) | TF(CO$_2$)[b] total | [H$_2$] ($\times 10^{-5}$ mol) | TF(H$_2$)[b] | [MH][c] ($\times 10^{-5}$ mol) | TF(MH)[b,c] | [Heptanal] ($\times 10^{-5}$ mol) | [1,1-DMH][d] ($\times 10^{-5}$ mol) |
|---|---|---|---|---|---|---|---|---|
| 100 | 143.0 | 172 | 46.3 | 55 | 38.2 | 46 | 22.3 | 74.0 |
| 110 | 172.1 | 207 | 53.0 | 64 | 42.0 | 50 | 15.1 | 103.0 |
| 120 | 195.0 | 234 | 61.2 | 73 | 44.0 | 53 | 9.0 | 123.1 |
| 130 | 213.3 | 256 | 77.5 | 92 | 51.2 | 61 | 24.3 | 108.0 |
| 140 | 230.0 | 276 | 97.0 | 117 | 57.1 | 69 | 48.0 | 82.2 |

[a] $[Rh] = 0.022$ g $(5 \times 10^{-5}$ mol), [1-hexene] $= 0.4$ mL $(3 \times 10^{-3}$ mol), 1-hexene/Rh = 64, 10 mL (0.24 mol) of methanol, $P(CO) = 25$ atm for 4 h.

[b] TF(product) = [(mol of product/mol of Rh) × rt] × 24 h, where rt = reaction time in hours. Experimental uncertainty < 10%.
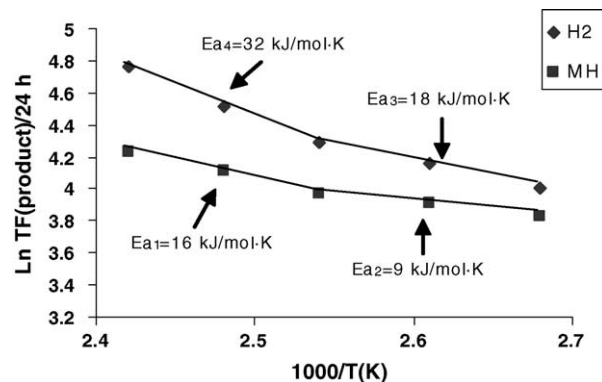
[c] MH = methyl-heptanoate.

[d] DMH = dimethoxy-heptane.

Table 4

The effect of the Rh concentration variation on WGSR, hydroesterification and hydroformylation–acetalization of 1-hexene in methanol, catalyzed by the $cis$-[Rh(CO)$_2$(4-pic)$_2$](PF$_6$) complex[a]

| [Rh] ($\times 10^{-5}$ mol) | [CO$_2$] (total) ($\times 10^{-5}$ mol) | TF(CO$_2$)[b] total | [H$_2$] ($\times 10^{-5}$ mol) | TF(H$_2$)[b] | [MH][c] ($\times 10^{-5}$ mol) | TF(MH)[b,c] | [Heptanal] ($\times 10^{-5}$ mol) | [1,1-DMH][d] ($\times 10^{-5}$ mol) |
|---|---|---|---|---|---|---|---|---|
| 1 | 62.0 | 74 | 36.9 | 220 | 15.2 | 91 | 16.0 | 10.1 |
| 5 | 281.2 | 337 | 172.1 | 206 | 64.0 | 76 | 67.2 | 45.2 |
| 10 | 498.3 | 598 | 282.0 | 170 | 97.2 | 59 | 120.3 | 69.0 |
| 20 | 818.9 | 983 | 490.2 | 147 | 161.0 | 48 | 213.0 | 118.4 |
| 30 | 1040.0 | 1248 | 670.4 | 132 | 188.0 | 38 | 213.1 | 137.0 |

[a] [1-Hexene] = (0.1–3.7) mL ((0.8–30 $\times 10^{-3}$) mol), S/C = 100, 10 mL (0.24 mol) of methanol, $P$(CO) = 25 atm at 100 °C for 4 h.

[b] TF(product) = [(mol of product/mol of Rh) $\times$ rt] $\times$ 24 h, where rt = reaction time in hours. Experimental uncertainty < 10%.

[c] MH = methyl-heptanoate.

[d] DMH = dimethoxy-heptane.

($3 \times 10^{-3}$ mol), 1-hexene/Rh = 64, 10 mL (0.24 mol) of methanol, $P$(CO) = 25 atm for 4 h. The Arrhenius plot of ln TF(MH)/(24 h$^{-1}$) values versus $1/T$ was nonlinear in the 100–140 °C range, giving segmented curves. The apparent activation energies obtained from the slopes of the two segments are 9 kJ/mol K at temperatures < 120 °C and 16 kJ/mol K at temperatures > 120 °C. On the other hand, the apparent activation energies obtained from the slopes of the two segments for the hydrogen production are 18 kJ/mol K at temperatures < 120 °C and 32 kJ/mol K at temperatures > 120 °C. Arrhenius plots that are segmented indicate a change in the rate-limiting step between competitive reactions [24]. Other factors such as variation of the oxidation state of catalytic active species may be responsible for curvatures in Arrhenius plots [25].

As shown in Table 3, varying the temperature from 100 to 140 °C, increases the production of H$_2$, CO$_2$ and methyl-heptanoate and decreases the production of 1,1-dimethoxy-heptane at $T$ > 120 °C. Similar tendencies for WGSR results were observed for the [Rh(cod)(4-pic)$_2$](PF$_6$) (cod = 1,5-cyclooctadiene) immobilized on poly(4-vinylpyridine) in carbon monoxide atmosphere (1 bar) on the 100–180 °C range under continuous-flow conditions [25].

### 3.4.3. Effect of the Rh concentration

Catalytic runs were carried out for a series of different rhodium concentrations over the range (1–30) $\times 10^{-5}$ mol (Table 4). A typical run involved determination of TF/24 h as a function of [Rh] at [methanol] = 10 mL, 1-hexene/Rh = 100 under $P$(CO) = 25 atm at 140 °C (under this temperature, the production of methyl-heptanoate reaches the highest value (Table 3). The amount of 1-hexene was varied from 0.1 mL (0.8 $\times 10^{-3}$ mol) at [Rh] = 1 $\times 10^{-5}$ mol to 3.7 mL (30 $\times 10^{-3}$ mol) at [Rh] = 30 $\times 10^{-5}$ mol in order to keep the ratio [1-hexene]/[Rh] = 100 in all runs (Table 4). Fig. 3 shows the plot of TF(MH)/24 h and TF(H$_2$)/24 h values versus [Rh].

An increase in [Rh] from (1 to 10) $\times 10^{-5}$ mol resulted in a decrease in both TF(MH)/24 h and TF(H$_2$)/24 h, followed by nearly constant values at higher [Rh] (Fig. 3). The results indicate that reaction rate is not first order for both reactions in the [Rh] (1–30) $\times 10^{-5}$ mol range, and suggest that the active species may be present in several forms having different nuclearity (mononuclear and polynuclear). This suggestion is strongly supported by the FT-IR and X-ray data reported for the soluble Rh(py)$_2$ WGSR catalysts system, which show the presence of rhodium species with different nuclearity (mononuclear and polynuclear) and oxidation state ((I) and (−I)). The Rh(−I) specie comes from the reduction of $cis$-[Rh(CO)$_2$(py)$_2$]$^+$ by CO/H$_2$O to CO$_2$ and [(py)$_2$H][Rh$_5$(CO)$_{13}$(py)$_2$] complex, which was structurally characterized [26]. Hence, a catalytic cycle for the WGSR was proposed where $cis$-[Rh(CO)$_2$(py)$_2$]$^+$ and [Rh$_5$(CO)$_{13}$(py)$_2$]$^-$ are the active species [27]. Further, mechanistic studies for WGSR catalyzed by Rh(amine)$_2$ complexes dissolved in aqueous amine suggest a nucleophilic attack by water on the coordinated CO, assisted by free pyridine. This yields hydroxycarbonyl Rh specie and protonated amine as a fundamental step [13]. The negative charge of the anionic polynuclear complex (−I) increases the energy of this step and diminishes the catalytic activity.

### 3.4.4. Effect of the 1-hexene/Rh molar ratio

The effect of varying the 1-hexene/Rh molar ratio on the 64–500 range for the Rh(4-pic)$_2$ catalytic system under the condition described in Table 5 was studied. The TF(MH) increases from 67 (24 h$^{-1}$) at [1-hexene] = 0.4 mL ($3 \times 10^{-3}$ mol), reaching a maximum value of 76 (24 h$^{-1}$) at [1-hexene] = 0.6 mL (4.5 $\times 10^{-3}$ mol) and then decreases to 48 (24 h$^{-1}$) at [1-hexene] = 3.0 mL (25 $\times 10^{-3}$ mol). The
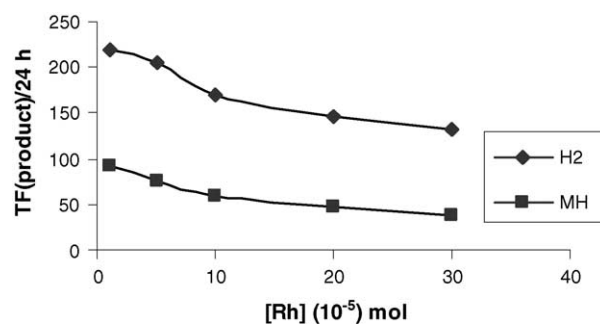


Fig. 3. A plot of TF(product)/24 h vs. [Rh]: (♦) hydrogen and (■) methyl heptanoate. Reaction conditions: [1-hexeno] = 0.1–3.7 mL ((0.8–30) $\times 10^{-3}$ mol), S/C = 100, 10 mL (0.24 mol) of methanol, $P$(CO) = 25 atm at 100 °C for 4 h. Lines drawn for illustrative purpose only.

Table 5
The effect of the 1-hexene/Rh molar ratio (S/C) variation on WGSR, hydroesterification and hydroformylation–acetalization of 1-hexene in methanol, catalyzed by the *cis*-[Rh(CO)$_2$(4-pic)$_2$](PF$_6$) complex[a]

| S/C molar ratio | [CO$_2$] (total) ($\times 10^{-5}$ mol) | TF(CO$_2$)[b] total | [H$_2$] ($\times 10^{-5}$ mol) | TF(H$_2$)[b] | [MH][c] ($\times 10^{-5}$ mol) | TF(MH)[b,c] | [Heptanal] ($\times 10^{-5}$ mol) | [1,1-DMH][d] ($\times 10^{-5}$ mol) |
|---|---|---|---|---|---|---|---|---|
| 64 | 230.0 | 276 | 97.3 | 117 | 56.1 | 67 | 48.3 | 82.0 |
| 100 | 281.0 | 337 | 172.0 | 206 | 63.0 | 76 | 67.2 | 45.3 |
| 250 | 375.4 | 451 | 245.0 | 294 | 52.0 | 62 | 65.0 | 60.4 |
| 500 | 432.2 | 519 | 299.2 | 359 | 40.2 | 48 | 60.1 | 75.1 |

[a] [Rh] = 0.022 g ($5 \times 10^{-5}$ mol), [1-hexene] = 0.4 mL ($3 \times 10^{-3}$ mol) to 3.0 mL ($25 \times 10^{-3}$ mol), 10 mL (0.24 mol) of methanol, $P$(CO) = 25 atm at 140 °C for 4 h.

[b] TF(product) = [(mol of product/mol of Rh) × rt] × 24 h, where rt = reaction time in hours. Experimental uncertainty < 10%.
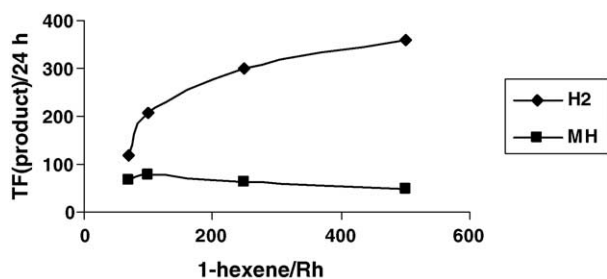
[c] MH = methyl-heptanoate.

[d] DMH = dimethoxy-heptane.



Fig. 4. A plot of TF(product)/24 h vs. 1-hexene/Rh molar ratio: (♦) hydrogen and (■) methyl heptanoate. Reaction conditions: [Rh] = 0.022 g ($5 \times 10^{-5}$ mol), [1-hexene] = 0.4 mL ($3 \times 10^{-3}$ mol) to 3.0 mL ($25 \times 10^{-3}$ mol), 10 mL (0.24 mol) of methanol, $P$(CO) = 25 atm at 140 °C for 4 h. Lines drawn for illustrative purpose only.

plot of TF(MH)/24 h values versus 1-hexene/Rh molar ratio shown in Fig. 4 indicates a reversible addition of 1-hexene to rhodium center on the 1-hexene/Rh (64–400) molar ratio range. On the other hand, at S/C = 500 molar ratio, the hydroformylation–acetalization reaction is more favored than hydroesterification. Contrary to what is expected, the WGSR is favored at high 1-hexene concentration. Maybe, the observed reversible coordination of 1-hexene to Rh center at high olefin concentration switches the reaction to the WGSR side (see Scheme 1).

### 3.4.5. Effect of the reaction medium

The catalytic hydroesterification and hydroformylation–acetalization of 1-hexene by Rh(4-pic)$_2$ system was also carried out in methanol/water, ethanol, and ethanol/water mixtures (Table 6). Under the following reaction conditions: [Rh] = 0.022 g ($5 \times 10^{-5}$ mol), [1-hexene] = 0.4 mL ($3 \times 10^{-3}$ mol), 1-hexene/Rh = 64; 10 mL of ethanol or 10 mL of ethanol/water 8/2 (v/v), under $P$(CO) = 0.9 atm at 100 °C for 4 h. The GC and GC–mass analyses of the liquid phase runs allowed the identification and quantification of ethyl-heptanoate, heptanal and 1,1-diethoxy-heptane, coming from 1-hexene hydroesterification, hydroformylation
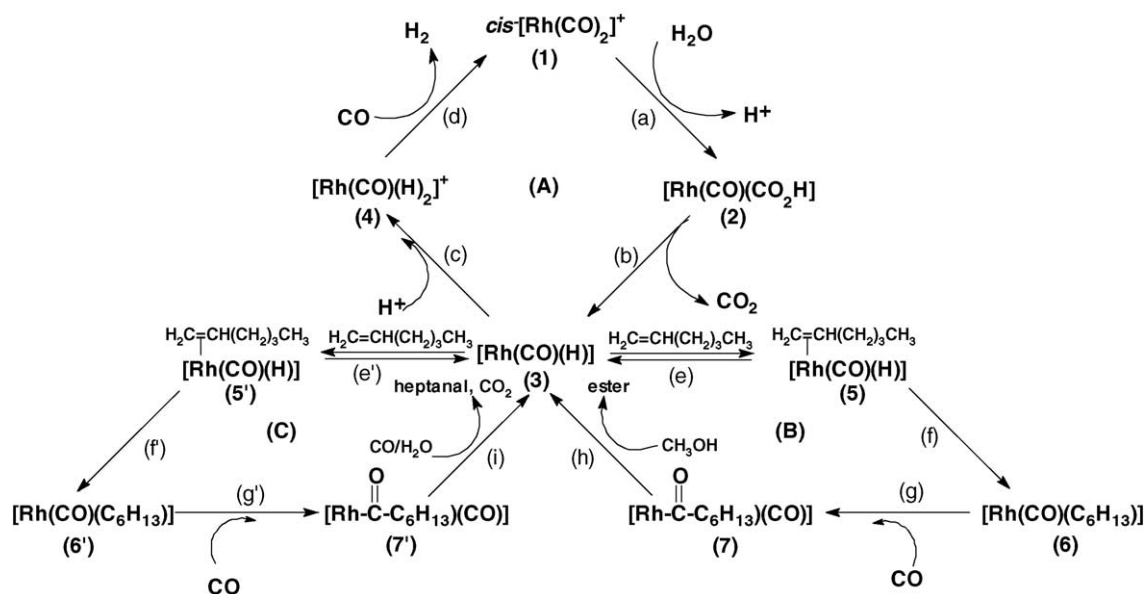


Scheme 1. Proposed mechanism.

Table 6
The effect of the reaction medium variation on WGSR, hydroesterification and hydroformylation–acetalization of 1-hexene, catalyzed by the cis-[Rh(CO)$_2$(4-pic)$_2$](PF$_6$) complex[a]

| Reaction medium | [CO$_2$] (total) ($\times 10^{-5}$ mol) | TF(CO$_2$)[b] total | [H$_2$] ($\times 10^{-5}$ mol) | TF(H$_2$)[b] | [MH][c] ($\times 10^{-5}$ mol) | TF(MH)[b,c] | [Heptanal] ($\times 10^{-5}$ mol) | [1,1-DMH][d] ($\times 10^{-5}$ mol) |
|---|---|---|---|---|---|---|---|---|
| Methanol | 12.5 | 15 | 4.8 | 5 | 11.8 | 14 | 0.2 | 7.5 |
| Ethanol | 12.5 | 19 | 5.2 | 6 | 7.5 | 9 | 2.5 | 2.2 |
| Methanol/water (8/2) | 11.0 | 28 | 4.0 | 5 | 7.5 | 9 | 2.3 | 4.5 |
| Ethanol/water (8/2) | 25.6 | 45 | 5.8 | 7 | 6.1 | 7 | 7.9 | 11.5 |

[a] [Rh] = 0.022 g (5 $\times 10^{-5}$ mol), [1-hexene] = 0.4 mL (3 $\times 10^{-3}$ mol), 1-hexene/Rh = 64; 10 mL of solvent system, P(CO) 0.9 atm at 100 °C for 4 h.
[b] TF(product) = [mol of product/mol of Rh) $\times$ rt] $\times$ 24 h, where rt = reaction time in hours. Experimental uncertainty < 10%.
[c] MH = methyl-heptanoate.
[d] DMH = dimethoxy-heptane.

and nucleophilic addition reaction between ethanol and the formed heptanal, respectively (see Table 6). Also the system in sole ethanol, ethanol/water or methanol/water catalyzed the WGSR. These results are almost similar to those observed for the Rh(4-pic)$_2$/methanol system described above under similar reaction conditions. Accordingly, for the hydroesterification of 1-hexene by the Rh(4-pic)$_2$ complex in contact with methanol or ethanol, the carbon chain length of the aliphatic alcohols has little influence on the reaction rate in accordance with earlier reports [28–30]. Analyses of the effects of varying the nature of coordinated amine on the catalytic hydroesterification of 1-hexene in methanol/water, ethanol and ethanol/water mixtures are in progress.

Further, the catalytic hydroesterification of 1-hexene in methanol was reproduced under optimal conditions (as determined from Tables 2–5, e.g. [Rh] = 1 $\times 10^{-5}$ mol, 10 mL (0.24 mol) of methanol, 1-hexene/Rh = 100 and P(CO) = 25 atm at 140 °C for 4 h) furnishing the highest TF(MH) value, ca. 91 (24 h$^{-1}$). No attempts were made to recycle the catalyst under these conditions due to formation of some insoluble material after liquid phase removal by distillation.

### 3.5. Mechanistic considerations

Scheme 1 illustrates a proposed mechanism for the WGSR and the hydroformylation and hydroesterification reaction of 1-hexene by the highly and stable Rh(4-pic)$_2$ system. The evaluation of the mechanism for H$_2$, CO$_2$, methyl-heptanoate and heptanal formation by this catalytic system under CO shows a few key features.

First, the rhodium(I) cis-[Rh(CO)$_2$(amine)$_2$](PF$_6$) (amine = 4-picoline or pyridine) complexes in 80% aqueous amine, under 0.9 atm of CO at 100 °C, catalyzed the water gas shift reaction. Proposed mechanisms for these systems involve the formation of rhodium hydride intermediates, which were confirmed by in situ $^1$H NMR spectroscopic studies [13]. Further, FT-IR and X-ray studies [24], showed the presence of mononuclear cationic Rh(I) and polynuclear anionic carbonyl Rh(−I) compounds as reaction intermediates in the WGSR, which probably are formed in the present system.

Second, the CO$_2$ turnover frequencies in the presence of 1-hexene for the Rh(amine)$_2$ systems are greater than the WGSR activity for the same system in the absence of 1-hexene. Presumably in the former systems a reactive Rh–H intermediate is intercepted prior to H$_2$ formation by reaction with 1-hexene to generate a rhodium–olefin intermediate. Under WGSR conditions the latter would expect to react further to give the observed organic products.

Third, the studies of the variation of [Rh] also suggest the occurrence of mono–polynuclear equilibrium between active rhodium species having different nuclearity, under the catalytic conditions.

Fourth, a blank experiment using H$_2$/CO (synthesis gas) as an alternative to CO/H$_2$O was carried out in order to examine the possibility that molecular H$_2$ (coming from the WGSR) in presence of CO and 1-hexene forms heptanal under the catalytic conditions described in Tables 1-5. Therefore, a mixture of 0.022 g (5 $\times 10^{-5}$ mol) of cis-[Rh(CO)$_2$(4-pic)$_2$](PF$_6$), 1.24 mL (1 $\times 10^{-2}$ mol) of 1-hexene and 10 mL of pre-dried 2-ethoxyethanol was added to a 150 mL glass reactor vessel, and then was degassed by three freeze–pump–thaw cycles. The reaction vessel was charged with a CO/H$_2$ mixture (P(H$_2$) = 0.9 and P(total) = 1.8 atm) at 100 °C for 5 h. GC and GC–mass analyses of the liquid phase revealed the presence of 2-hexene and 3-hexene as the only organic products which come from the catalytic isomerization of 1-hexene. Heptanal was not formed or detected in the reaction mixture. Consequently, the Rh(4-pic)$_2$ system does not catalyze the hydroformylation–acetalization of 1-hexene to heptanal or 1,1-dimethoxy-heptane under CO/H$_2$ with these reaction conditions. This result strong suggests that the H$_2$ formed under CO/H$_2$O system does not further react with 1-hexene. On the other hand, pre-dried 2-ethoxyethanol was used as medium system because it does not dehydrate under the reaction conditions described above.

Given the above, the reaction mechanism depicted in Scheme 1 is proposed for WGSR, hydroesterification and hydroformylation of 1-hexene catalyzed by mononuclear cationic Rh(I) species. In Scheme 1, the amine ligands of the intermediate rhodium are omitted for clarity. Three connected cycles account for the observed products. In cycle (A), the formation of H$_2$ via WGSR implies a nucleophilic attack by H$_2$O on the coordinated CO of complex **1** to yield

a hydroxycarbonylation complex [Rh(CO)(CO$_2$H)] (**2**) and H$^+$ (step a). Elimination of CO$_2$ from the former complex gives the hydride [Rh(CO)H] complex **3** (step b), which upon protonation by H$^+$ (step c) forms the dihydride complex [Rh(CO)(H)$_2$]$^+$ (**4**). Reductive elimination of H$_2$ (step d) assisted by CO coordination regenerates the starting [Rh(CO)$_2$]$^+$ complex **1** and closes the WGSR cycle.

Cycle (B) describes the formation of methyl-heptanoate (ester) which comes from in situ methanolysis of the [Rh(CO)(acyl)] complex **7** (step h). The Rh–acyl complex arises from coordination of 1-hexene to form the intermediate complex **5** (step e). Insertion of the olefin to the Rh–H bond (step f) [31] gives [C$_6$H$_{13}$Rh(CO)] (**6**). Then *cis*-migration of the C$_6$H$_{13}$ group so formed to [Rh–CO] moiety assisted by CO coordination (step g) gives the [Rh(CO)(acyl)] complex **7**. Formation of the hydride-rhodium complex **3** and production of methyl-heptanoate (step h) closes the catalytic cycle (B). The results in Section 3.2 show the production of methyl-heptanoate as a function of the p$K_a$ value of the coordinated amine. The electron-donating methyl groups on the pyridine ring increase the nucleophilicity of the Rh center and favor the electrophilic attack by the acidic H of methanol over the metal center and facilitates [Rh(CO)(H)] (**3**) formation. Simultaneously, the nucleophilic attack by the oxygen atom of CH$_3$O group of methanol over the electrophilic carbonyl carbon of acyl ligand facilitates ester formation, hence increasing the methanolysis reaction (step h).

Cycle (C) describes the formation of heptanal which came from in situ hydrogenolysis of Rh–acyl complex **7'** (step i). Hydrogenolysis of the Rh-acyl intermediate, which leads to heptanal formation, probably comes from *intra*-hydrogen transfer from Rh–H species formed under conditions similar to the WGSR (cycle A). Namely, nucleophilic attack by OH$^-$ on a coordinated carbonyl ligand of the [Rh(CO)(acyl)] complex would afford the anionic rhodium hydroxycarbonyl [Rh(CO$_2$H)(acyl)]$^-$ complex and H$^+$, Eq. (9):

$$[Rh(CO)(acyl)] + H_2O \rightarrow [HRh(CO_2H)(acyl)]^- + H^+ \quad (9)$$
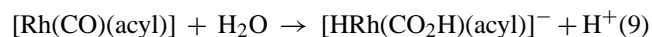
Decarboxylation of rhodium hydroxycarbonyl intermediate would generate a rhodium hydride complex [HRh(acyl)]$^-$ and CO$_2$ (Eq. (10)):
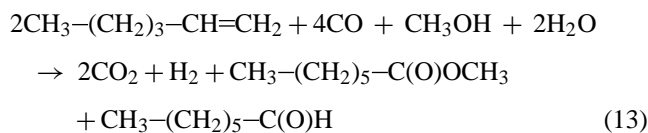
$$[Rh(CO_2H)(acyl)]^- \rightarrow [HRh(acyl)]^- + CO_2 \quad (10)$$
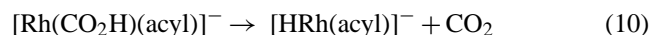
Reductive elimination of hydride-acyl complex assisted by CO coordination affords heptanal and a coordinatively unsaturated [Rh(CO)]$^-$ complex according to Eq. (11). The negative charge accumulation on the hydride–acyl complex favors the migration of coordinated H to Rh–C bond [31]:

$$[HRh(acyl)]^- + CO \rightarrow [Rh(CO)]^- + heptanal \quad (11)$$

Protonation of the latter anionic complex by H$^+$ (Eq. (12)) would give the starting [Rh(CO)(H)] complex **3** to close cycle (C):

$$[Rh(CO)]^- + H^+ \rightarrow [Rh(CO)(H)] \quad (12)$$

The overall reaction for products formation is (Eq. (13)):

$$2CH_3-(CH_2)_3-CH=CH_2 + 4CO + CH_3OH + 2H_2O$$
$$\rightarrow 2CO_2 + H_2 + CH_3-(CH_2)_5-C(O)OCH_3$$
$$+ CH_3-(CH_2)_5-C(O)H \quad (13)$$

Eq. (13) does not include the side product, 1,1-dimethoxy-heptane, which is principally formed in stoichiometric fashion.

Furthermore, the TF(MH) = 14 (24 h$^{-1}$) value, for the "Rh(4-pic)$_2$" system, is higher than the TF(heptanal) = 10.8 (24 h$^{-1}$) value, by a factor of 1.3. The calculated TF(heptanal) value reported here is based on total amount of CO$_2$ formed (TF(CO$_2$)$_{tot}$ = 15, Eqs. (4) and (5)) minus the amount of CO$_2$ (H$_2$) coming from the WGSR (TF(H$_2$) = 5 (24 h$^{-1}$)), keeping that CO$_2$/H$_2$ molar ratio is equal to **1** according to Eq. (5). These results show, that the termination step by methanolysis of **6** affording methyl-heptanoate (step h) is faster than the termination step by hydrogenolysis of **6'** affording heptanal (step i), in spite of the fact that both products come from the same kind of intermediates, namely the Rh–acyl complexes **7** and **7'**. However, methanol is in a much higher concentration than water. Accordingly, the methanolysis reaction is the rate determining step. It is also well known that hydroesterification of olefins is slower than hydroformylation [1]. Analogous cycle may be proposed for the polynuclear complexes.

Experiments related to the catalytic reaction of the other olefins present in a typical naphtha, in particular cyclohexene (11.4 wt.%) and 2-methyl-2-pentene together with 2,3-dimethyl-1-butene (56.6 wt.%) by these Rh systems are in progress.

## 4. Conclusions

In this work we carried out the catalytic transformation of 1-hexene, which is present in about 33% among the olefins in the LSR, in oxygenated compounds (esters and aldehyde-acetals) under CO atmosphere. This approximation constitutes a promising work for a future industrial catalytic process for gasoline improving based on Reppe type reaction. Methyl-heptanoate, heptanal and 1,1-dimethoxy-heptane were synthesized by the hydroesterification and hydroformylation–acetalization of 1-hexene. The above reactions were catalyzed by soluble *cis*-[Rh(CO)$_2$(amine)$_2$](PF$_6$) complexes in methanol under carbon monoxide atmosphere. Formation of 1,1-dimethoxy-heptane comes principally from the nucleophilic addition reaction between methanol and catalytic formed heptanal. Further, these Rh(amine)$_2$ catalytic systems are active for the WGSR under the hydroesterification and hydroformylation–acetalization reaction conditions. The electronic factor of the coordinated amine influences the rate. In particular, the Rh(2,6-lut)$_2$ system shows to be the most active among the amine-catalysts

tested toward the hydroesterification compared with the hydroformylation–acetalization reactions. The opposite is observed for the less basic pyridines. The increment of the $P(CO)$ favors the WGSR and hydroformylation–acetalization activities but disfavors the hydroesterification reaction.

Based on temperature and Rh concentration dependence and previous characterization studies, it can be suggested that the observed segmentation in the Arrhenius-type plot is the result of the hydroesterification catalyzed by both mononuclear and polynuclear carbonylrhodium complexes of 4-picoline ligand, with different energy pathways.

Finally, a catalytic scheme for the production of $H_2$, $CO_2$, methyl-heptanoate and heptanal bearing common Rh–H catalytic species is proposed.

## Acknowledgments

## References

[1] P. Pino, F. Piacenti, M. Bianchi, in: I. Wender, P. Pino (Eds.), Organic Synthesis via Metal Carbonyls, John Wiley, New York, 1968, p. 233.
[2] G. Kiss, Chem. Rev. 101 (2001) 3435.
[3] M. Kilner, N.J. Winter, J. Mol. Catal. A 112 (1996) 327.
[4] M.M. Mdleleni, R.G. Rinker, P.C. Ford, J. Mol. Catal. 89 (1994) 283.
[5] M.M. Mdleleni, R.G. Rinker, P.C. Ford, Inorg. Chim. Acta 270 (1998) 345.
[6] A.J. Pardey, C. Longo, T. Funaioli, G. Fachinetti, Polyhedron 23 (2004) 1677.
[7] A. Cabrera, P. Sharma, J.L. Garcia, L. Velazco, F.J. Perez, J.L. Arias, N. Rosas, J. Mol. Catal. A 118 (1997) 167.
[8] G. Verspui, J. Feiken, G. Papadogianaskis, R.A. Sheldon, J. Mol. Catal. A 146 (1999) 299.
[9] A.J. Pardey, A.B. Rivas, C. Longo, T. Funaioli, G. Fachinetti, J. Coord. Chem. 57 (2004) 871.
[10] P.W.N.M. van Leeuwen, C. Claver, Rhodium Catalyzed Hydroformylation, Kluwer/Academia Publishers, New York, 2000.
[11] B. El Ali, J. Tijani, M. Fettouhi, J. Mol. Catal. A 230 (2005) 9 (and references therein).
[12] D. Little, Catalytic Reforming, Pem Wel Publishing, 1958.
[13] A.J. Pardey, P.C. Ford, J. Mol. Catal. 53 (1989) 247.
[14] N. Kumari, M. Sharma, P. Das, D.K. Dutta, Appl. Organomet. Chem. 16 (2002) 258.
[15] C. Linares, M. Mediavilla, A.J. Pardey, P. Baricelli, C. Longo-Pardey, S.A. Moya, Catal. Lett. 50 (1998) 183.
[16] A.J. Pardey, C. Longo, T. Funaioli, G. Fachinetti, Polyhedron 23 (2004) 1683.
[17] B. Denise, G. Pannetier, J. Organomet. Chem. 63 (1973) 423.
[18] C. Longo, J. Alvarez, M. Fernández, A.J. Pardey, S.A. Moya, P. Baricelli, M.M. Mdleleni, Polyhedron 19 (2000) 487.
[19] H.M. McNair, J.M. Miller, Basic Gas Chromatography, Wiley/Interscience, New York, 1997 (Chapter 8).
[20] Yu.T. Vigranenko, S.Yu. Sukov, Russ. J. Appl. Chem. 72 (1999) 247.
[21] K. Schofield, Hetero-Aromatic Nitrogen Compounds, Plenum Press, New York, 1967, pp. 146–148.
[22] R.T. Morrison, R.N. Boyd, Organic Chemistry, 3rd ed., Allyn and Bacon, Boston, 1973, p. 631.
[23] P.C. Ford, A. Rokicki, Adv. Organometal. Chem. 28 (1988) 139.
[24] A.A. Frost, R.G. Pearson, Kinetics and Mechanism, Wiley, New York, 1961, p. 24.
[25] A.J. Pardey, M. Fernández, J. Alvarez, C. Urbina, D. Moronta, V. Leon, M. Haukka, T.A. Pakkanen, Appl. Catal. A 199 (2000) 275.
[26] G. Fachinetti, T. Funaioli, P.F. Zanazzi, J. Organometal. Chem. 460 (1993) 34.
[27] G. Fachinetti, G. Fochi, T. Funaioli, Inorg. Chem. 33 (1994) 1719.
[28] J.F. Knifton, J. Org. Chem. 41 (1976) 2885.
[29] J.F. Knifton, J. Am. Oil Chem. Soc. 55 (1978) 496.
[30] G. Cavinato, L. Toniolo, J. Mol. Catal. A 104 (1996) 221.
[31] G. Consiglio, Chimia 55 (2001) 809.